Interaction of HTLV-1 Tax with minichromosome maintenance proteins accelerates the replication timing program

Mathieu Boxus,[1] Jean-Claude Twizere,[1] Sébastien Legros,[1] Richard Kettmann,[1] and Luc Willems[1,2]

[1]National Fund for Scientific Research, Gembloux Agro-Bio Tech, Cellular and Molecular Biology, University of Liège, Liège, Belgium; and [2]Interdisciplinary Cluster for Applied Genoproteomics, University of Liège, Liège, Belgium

The Tax oncoprotein encoded by the human T-cell leukemia virus type 1 plays a pivotal role in viral persistence and pathogenesis. Human T-cell leukemia virus type 1–infected cells proliferate faster than normal lymphocytes, expand through mitotic division, and accumulate genomic lesions. Here, we show that Tax associates with the minichromosome maintenance MCM2-7 helicase complex and localizes to origins of replication. Tax modulates the spatiotemporal program of origin activation and fires supplementary origins at the onset of S phase. Thereby, Tax increases the DNA replication rate, accelerates S phase progression, but also generates a replicative stress characterized by the presence of genomic lesions. Mechanistically, Tax favors p300 recruitment and histone hyperacetylation at late replication domains, advancing their replication timing in early S phase. (*Blood*. 2012;119(1):151-160)

Introduction

Human T-cell leukemia virus-1 (HTLV-1) is a retrovirus that infects approximately 20 million people worldwide.[1] Although the majority of infected people remain lifelong asymptomatic carriers, 2% to 5% develop either adult T-cell leukemia (ATL) or chronic inflammatory diseases, such as HTLV-1–associated myelopathy/tropical spastic paraparesis.[1] Two major hallmarks of HTLV-1–infected cells are: preferential proliferation compared with normal lymphocytes[2] and tendency to accumulate genomic lesions, a prerequisite for oncogenesis.[3,4]

Although the molecular mechanisms underlying T-cell transformation remain to be elucidated, it is generally accepted that the virally encoded Tax protein plays a central role. Tax indeed displays pleiotropic activities that cooperate to drive cell cycle progression and perturb genome stability.[4,5] For example, Tax shortens G_1 phase and accelerates transition into S phase by manipulating positive and negative G_1 phase regulators (ie, cyclin D/CDK complex, Rb and CDK inhibitors).[6-8] In addition, Tax is thought to indirectly generate DNA damage by suppressing DNA repair processes and competing with cellular DNA damage response (DDR).[4,5] Recent data also support a direct role for Tax-induced reactive oxygen species in the occurrence of DNA lesions.[9]

Conceptually, Tax activities are achieved through protein-protein interactions in both nuclear and cytoplasmic cellular compartments.[10] In the nucleus, Tax accumulates within foci called Tax speckled structures (TSS),[11] which overlap with the cellular machinery required for transcription, splicing, post-transcriptional modifications of proteins, DNA repair, and checkpoint control.[12]

In this report, we further demonstrate that Tax recruits the MCM2-7 replicative helicase within the TSS and modulates the program of replication origin firing. Notably, this mechanism favors cell cycle progression and directly compromises genome stability.

Methods

Plasmids, antibodies, yeast 2-hybrid, and GST pulldown

See supplemental Methods (available on the *Blood* Web site; see the Supplemental Materials link at the top of the online article).

Cell culture

HeLa, Rat-1, and 293GP2 cells were cultured in Dulbecco modified Eagle medium supplemented with 10% FBS and 2mM l-glutamine and penicillin/streptomycin. Jurkat, HUT78 and JPX9 (Jurkat cell lines stably transfected either with tax-1 gene driven by a metallothionein-inducible promoter) were kept in RPMI 1640 supplemented with 10% FBS, 2mM l-glutamine, and penicillin/streptomycin. Expression of the viral protein was induced in JPX9 cells by adding 120 μM zinc chloride ($ZnCl_2$) to the medium during at least 16 hours. HTLV-1–transformed T-cell lines (C91/PL, MT-2, MT4, C8166–45 and HUT102), ATL patient-derived (JuanaW, Champ, PaBe, StEd and ATL1), HTLV-1–associated myelopathy/tropical spastic paraparesis patient-derived cell lines (Eva and Xpos) have been provided by R. Grassmann (University Erlangen-Nürnberg, Erlangen, Germany) and cultured as previously described.[13]

HeLa and Rat-1 cells were transfected using Mirus Trans-IT LT1 reagent (Mirus Bio) as recommended by the manufacturer.

Where indicated, cells were synchronized at G_1/S border by adding 2mM hydroxyurea or 1 μg/mL aphidicolin in the medium during 16 hours. To inhibit ATM/ATR kinases, medium was supplemented with 2mM caffeine. For BrdU incorporation assays, cells were pulsed with 1μM BrdU during 30 minutes.

Stable cell lines

A total of 20 μg of lentiviral vectors (CSEF-IRES-bsd and pLKO.1-puro) was transfected in 2 million 293GP2 packaging cells together with 10 μg pCAG-HIVgp and 10 μg pCMV-VSV-G-RSV-Rev (provided by Masahiro Fujii, Niigata University, Japan) by the calcium chloride method to produce viral particles. Forty-eight hours after transfection, the media (10 mL) containing viral particles were recovered. A total of 1 million HeLa, JPX9,

Submitted May 26, 2011; accepted October 24, 2011. Prepublished online as *Blood* First Edition paper, November 4, 2011; DOI 10.1182/blood-2011-05-356790.

The online version of this article contains a data supplement.

The publication costs of this article were defrayed in part by page charge payment. Therefore, and solely to indicate this fact, this article is hereby marked "advertisement" in accordance with 18 USC section 1734.

or Rat-1 cells were infected 2 times, during 24 hours, with 5 mL of virus containing medium supplemented with polybrene (10 μg/mL). Cells were then washed and cultured in virus-free medium. After an additional overnight recovery, puromycin (2 μg/mL) or blasticidin (10 μg/mL) was added during 2 weeks.

Colony formation in soft agar

Rat-1 cells were stably infected with pCSEF-IB or pTax-IB, and pools of resistant cells (5×10^3 cells) were seeded in 0.33% agarose-containing DMEM-10% FCS overlaid on 0.5% agarose in a 24-well plate. After 3 weeks of culture, colonies were examined under light microscope and recovered from agarose.

Cell lysate preparation, cell fractionation, and Western blot

Cells were lysed for 20 minutes at 4°C with low salt (LB120; 0.1M Tris-Cl, pH 7.2, 120mM NaCl, 0.5% NP-40) or high salt lysis buffer (LB400; 0.1M Tris-Cl pH 7.2, 400mM NaCl, 0.5% NP-40) supplemented with Complete (Roche Diagnostics), 1mM Na_3VO_4, 0.1M NaF, and 1mM DTT. Where indicated, cells were extracted for 15 minutes at 4°C in cytoskeleton (CSK) buffer (10mM Pipes, pH 6.8, 100mM NaCl, 1.5mM $MgCl_2$, 300mM sucrose, 0.5% Triton X-100, Complete [Roche Diagnostics], 1mM Na_3VO_4, 0.1M NaF, 1mM DTT). Protein concentration was measured by the Bradford method (protein assay, Bio-Rad). Proteins (30 μg) were resolved by SDS-PAGE and analyzed by Western blotting using standard procedures. Bands were quantified with WCIF ImageJ Version 1.37b software (www.uhnresearch.ca/wcif/imagej/)

Coimmunoprecipitation

A total of 1×10^6 HeLa cells were seeded in 10-cm plates and transfected with 20 μg of plasmids. After 36 hours of incubation, cells were lysed in 1 mL of LB400 and centrifuged to eliminate debris. Lysates were diluted 3 times in LB buffer without salt. Equal amounts of lysates (500 μg) were incubated at 4°C for 2 hours with anti-Flag, anti-Tax or control antibodies under gentle shaking. Samples were then mixed with protein A/G agarose beads (Santa Cruz Biotechnology). After 1-hour incubation, beads were centrifuged and washed once in LB120, twice in LB400, and once in LB120 during 5 minutes under gentle shaking. Protein complexes were analyzed by Western blotting. A similar procedure was followed for coimmunoprecipitation of endogenous proteins.

ChIP and BrdU immunoprecipitation

JPX9 cells were treated with $ZnCl_2$ for 16 hours, and protein-DNA complexes were cross-linked with 1% paraformaldehyde for 10 minutes at 37°C. After quenching with 125mM glycine for 5 minutes, cells were washed with ice-cold PBS and resuspended in ChIP lysis buffer (Tris-Cl 50mM, pH 8.0, EDTA 10mM, SDS 1%) for 15 minutes at 4°C. DNA was sheared to a mean length of 500 bp (as estimated by agarose gel electrophoresis) using a Bioruptor sonifier (Diagenode), and lysates were cleared by centrifugation. ChIPs were performed with the OneDay ChIP Kit (Diagenode). Protein-DNA complexes were immunoprecipitated with 4 to 5 μg of antibody overnight. DNA was eluted according to the manufacturer's instructions and analyzed by quantitative PCR. BrdU immunoprecipitation was performed as described by Azuara.[14] Briefly, BrdU-pulsed JPX9 cells (50μM BrdU, 1 hour) were collected, washed, ethanol-fixed, and stained with propidium iodide (PI). A total of 30 000 cells were sorted with a FACSAria flow cytometer (BD Biosciences) in G_1, S_1, S_2, S_3, S_4, and G_2/M phases according to PI fluorescence. DNA was extracted with QiaAmp DNA extraction kit (QIAGEN) and sheared to a mean length of 500 bp using a Bioruptor sonifier (Diagenode). After heat denaturation (95°C, 5 minutes), BrdU-DNA was isolated by immunoprecipitation using an anti-BrdU monoclonal antibody (Sigma-Aldrich). After proteinase K digestion (15 minutes, 65°C), DNA was purified on a Qiaquick PCR purification column (QIAGEN) and analyzed by quantitative PCR. For ChIP and BrdU immunoprecipitation analysis, DNA was amplified with Mesa Green qPCR MasterMix Plus for SYBR Assay (Eurogentec) on a StepOne system (Applied Biosystems). Primers are listed in supplemental Table 1.

Fiber assay

Cells were pulsed with 40μM BrdU for 30 minutes, and DNA fiber spreads were prepared as described previously.[15] Cells (2000 cells/μL) were diluted (1:5) with unlabeled cells. A 2-μL aliquot was seeded on silanized glass slides followed by addition of 8 μL of lysis buffer (0.75% SDS, 200mM Tris-HCl, pH 7.4, and 50mM EDTA) and incubated for 5 minutes. DNA fibers were spread by tipping the slides at 20°. After migration down the slide, samples were fixed in methanol/acetic acid (3:1) for 10 minutes and allowed to dry. Slides were rehydrated with H_20 and incubated in 2.5M HCl for 30 minutes at 37°C to denature the DNA. Slides were briefly rinsed in TBS and incubated for 1 hour in blocking solution containing TBS, 1% (weight/volume) BSA, and 0.1% (volume/volume) Tween 20. Slides were incubated with monoclonal anti-BrdU (Sigma-Aldrich) in this buffer for 1 hour. Slides were washed several times in TBS plus Tween and labeled with goat anti–mouse IgG1–Alexa 488 and TOTO-3 (Invitrogen) diluted 1:1000 in blocking solution for 30 minutes. Samples were washed extensively in TBS and mounted in Gel Mount (Laborimpex). Random fields were selected using TOTO staining to ensure that only single DNA fibers (but not fiber bundles) were scored and recorded using a Zeiss fluorescence confocal microscope (Axiovert 200 with LSM 510) and a 63× (1.4 NA oil) objective. Fiber analysis was performed as described previously.[16,17]

Confocal microscopy

A total of 50 000 HeLa or Rat-1 cells were seeded onto glass coverslips disposed in 24-well plates, transfected with 1 μg of Tax-encoding vectors, and incubated for 16 hours. Where indicated, hydroxyurea (HU) was added 3 hours after transfection. Cells were then washed with PBS and, where indicated, pre-extracted with CSK buffer during 15 minutes at 4°C before fixation with 4% (weight/volume) paraformaldehyde in PBS for 20 minutes at room temperature. Cells were permeabilized with 0.5% (volume/volume) Triton X-100 in PBS for 15 minutes at room temperature. BrdU-stained cells were treated with 0.5% (volume/volume) Triton X-100 in 2N HCl during 30 minutes at room temperature. After several washes in PBS, cells were incubated during one hour with the appropriate primary antibodies diluted in immunofluorescence buffer (5% [volume/volume] FCS, 0.1% [volume/volume] Tween-20 in PBS). Cells were washed in immunofluorescence buffer and further incubated with the corresponding secondary antibodies. Where indicated, 5μM Draq5 reagent (Biostatus) was added during the last antibody incubation to stain cell nuclei. After 1-hour incubation, cells were washed extensively with immunofluorescence buffer, mounted in Gel Mount (Laborimpex), and processed for immunofluorescence using a Zeiss fluorescence confocal microscope (Axiovert 200 with LSM 510). Colocalization, fluorescence intensities, and particles analysis were performed using the WCIF ImageJ Version 1.37b software.

Flow cytometry

Transfected HeLa cells or zinc-stimulated Jurkat and JPX9 cells were collected and washed with cold PBS. Cells were fixed with ice-cold 70% ethanol or 4% PFA. BrdU-pulsed cells were further treated with 0.5% (volume/volume) Triton X-100 in 2N HCl during 30 minutes at room temperature. Cells were rinsed with wash buffer, incubated during 1 hour with appropriate primary antibodies, and labeled with the corresponding secondary antibodies during 30 minutes. For cell cycle analysis experiments, DNA was labeled with 4′,6-diamidino-2-phenylindole or PI after treatment of cells with RNAse A solution (0.1% [volume/volume] Tween-20, 10 μg/mL RNAse A in PBS). Labeled cells were analyzed with a FACSAria flow cytometer (BD Biosciences) using the Diva software. Rainbow beads (BD Biosciences) were used to check the linearity of the flow cytometer.

Determination of S phase length

Measurement of S phase length in Jurkat and JPX9 cells treated or not with $ZnCl_2$ was done as previously described.[18,19] Briefly, cells were pulsed with 33μM BrdU during 30 minutes, rinsed, resuspended in prewarmed and pregassed medium, and replaced in incubator. Cells were then collected at times (t) = 0, 2, 4, 6, and 8 hours, ethanol-fixed, and stained for BrdU and PI as mentioned above. Fraction of BrdU-labeled divided (f^{ld}) and undivided cells (f^{lu}), mean PI fluorescence of undivided BrdU labeled cells (F^{lu}), and cells with G_1 (F^{G1}) and G_2 (F^{G2}) DNA content were measured. Relative movement of BrdU-labeled cells at time t ($RM_{(t)}$) and duration of S (T_S) and G_2/M ($T_{G2/M}$) phases were computed as described previously.[19]

Statistical analysis

The data collected were analyzed using the GraphPad Prism Version 4.0 software. Statistical significance was calculated using Mann-Whitney or Kruskal-Wallis tests as indicated. The Spearman correlation test was used to examine the relationship between Tax expression and γH2AX levels. Data were considered significantly different when $P < .05$, $P < .01$, and $P < .001$.

Results

Tax interacts with the minichromosome maintenance protein complex and binds replication origins

To gain insight into the mechanisms involved in viral persistence and pathogenesis, we performed a yeast 2-hybrid screen using Tax as bait and isolated the MCM3 protein, a subunit of the MCM2-7 helicase, centrally involved in DNA replication processes. Coexpression of Gal4BD-Tax and Gal4AD-MCM3 fusion proteins promoted growth of the PJ696 yeast strain, indicating their physical interaction (supplemental Figure 1A). Consistently, GST pull-down and coimmunoprecipitation assays revealed that Tax complexes with MCM3-tagged proteins (supplemental Figure 1B-D; Figure 1A). The insensitivity of the interaction to the presence of ethidium bromide ruled out the possibility that DNA acts as a bridge between the 2 proteins (supplemental Figure 1E). In coimmunoprecipitation experiments, deletion of amino acids 2 to 22 (TaxΔ2-22) abrogated the interaction with MCM3 (Figure 1A). Importantly, this 2 to 22 deletion does not affect the zinc finger motif of Tax, required for its nuclear localization.[20,21] Tax was able to associate with endogenous members of the MCM2-7 complex but failed to bind other replication regulators, such as MCM10 or HBO1 (Figure 1B; and data not shown). The physiologic relevance of the interaction between Tax and endogenous MCM3 was further validated in HTLV-1–infected cell lines (Figure 1C).

MCM proteins mainly localize within the nucleus and associate with DNA replication origins.[22,23] Similarly, Tax is a predominantly nuclear protein that forms nuclear bodies, TSS.[11] In both control and Tax-expressing cells, MCM2 and MCM3 proteins showed a diffuse nuclear distribution that overlapped with TSS (Figure 1D; supplemental Figure 2). We also observed that wild-type Tax, but not the Δ2-22 mutant, recruits MCM2 protein phosphorylated at serine 27 (S27) or 41 (S41) within the nuclear bodies (Figure 1D; supplemental Figure 2). These 2 serines are targeted by Cdks/cyclins and/or Cdc7/Dbf4 during G_1/S, switching on the helicase at origins.[24,25] Labeling of DNA replication sites with BrdU in G_1/S synchronized cells further revealed that BrdU incorporation occurs in the periphery of the TSS (Figure 1D). Having established that Tax and MCMs colocalize within nuclear bodies and that nucleotide incorporation occurs at the surface of these structures, we checked whether Tax binds replication origins. Chromatin was immunoprecipitated from JPX9 cells (carrying a tax gene under the control of a zinc-inducible promoter) with anti-Tax antibodies. The abundance of DNA sequences spanning 6 well-defined replication origins (β-globin, Myc, LaminB2, FMR1 [fragile X mental retardation 1], TOP1, and RNF185) and 2 control regions (located 2 kb 5′ to the β-globin and Myc origins) was then measured by real-time PCR. As shown in Figure 1E, immunoprecipitation of Tax specifically increased the abundance of the 6 tested origins but not the 2 control regions (Ctrl). Notably, the Δ2-22 deletion abolished the ability of Tax to locate to replication origins (Figure 1F). MCM2-7 complex binds origins in late M and G_1 phases of the cell cycle.[22] ChIP experiments on chromatin prepared from zinc-stimulated JPX9 cells sorted into G_1, early S, late S, and G_2 population further demonstrated that Tax preferentially associates with origins in G_1 and early S phase of the cell cycle (Figure 1G).

Tax does not modulate licensing of replication origins

Association of Tax with MCM2-7 complex and replication origins suggested that the viral protein might impact on DNA replication processes. Initiation of DNA replication at an origin relies on a biphasic mechanism starting with the "licensing" of replication origins. This first step is characterized by the loading of MCM2-7 complexes on origins in late M and G_1 phases. The second step takes place at the onset of S phase and consists in the "firing" of licensed origins through activation of the MCM2-7 helicase.[22,23] During S phase, MCM proteins are progressively displaced from replication origins by moving ahead of the replication fork.[22,23]

To evaluate the effect of Tax on licensing, levels of chromatin-bound MCM2 and MCM3 were determined during the cell cycle of JPX9 cells. We used a flow cytometric approach providing a direct and quantitative measurement of global chromatin-bound levels of MCMs throughout cell cycle progression without cell synchronization.[26] A representative contour plot of chromatin-bound MCM3 versus DNA content (4′,6-diamidino-2-phenylindole) is shown in Figure 2A. Labeling of chromatin-bound MCM2 yielded similar patterns (data not shown). Mean fluorescence intensities (MFI) were measured in the G_1 and M phases of the cell cycle and normalized to the MFI of control cells in G_1. Tax expression in JPX9 cells did not affect the amounts of chromatin-bound MCM2/MCM3 in G_1 and M phases (Figure 2B). Similarly, ChIP experiments in G_1/S synchronized cells did not reveal differences of MCM2/MCM3 occupancy at defined origins on Tax expression (Figure 2C). These data suggest that Tax does not affect the licensing process per se.

Tax expression increases the number of replicon clusters and rates of DNA replication

Eukaryotic replication origins are organized in domains or clusters that fire synchronously at reproducible times throughout S phase. In a normal S phase, only approximately 10% of licensed origins initiate replication within a cluster, whereas others are inhibited through an ATR/CHK1-dependent control. These dormant origins are allowed to initiate only when DNA replication is compromised in active clusters.[16,17,27] To investigate whether Tax modulates firing of replication origins, we monitored nucleoside incorporation in control and Tax-expressing HeLa cells released from a G_1/S block. Tax caused a significant increase in the number of BrdU foci ($P < .001$; Figure 2E) but did not affect the fluorescence intensity

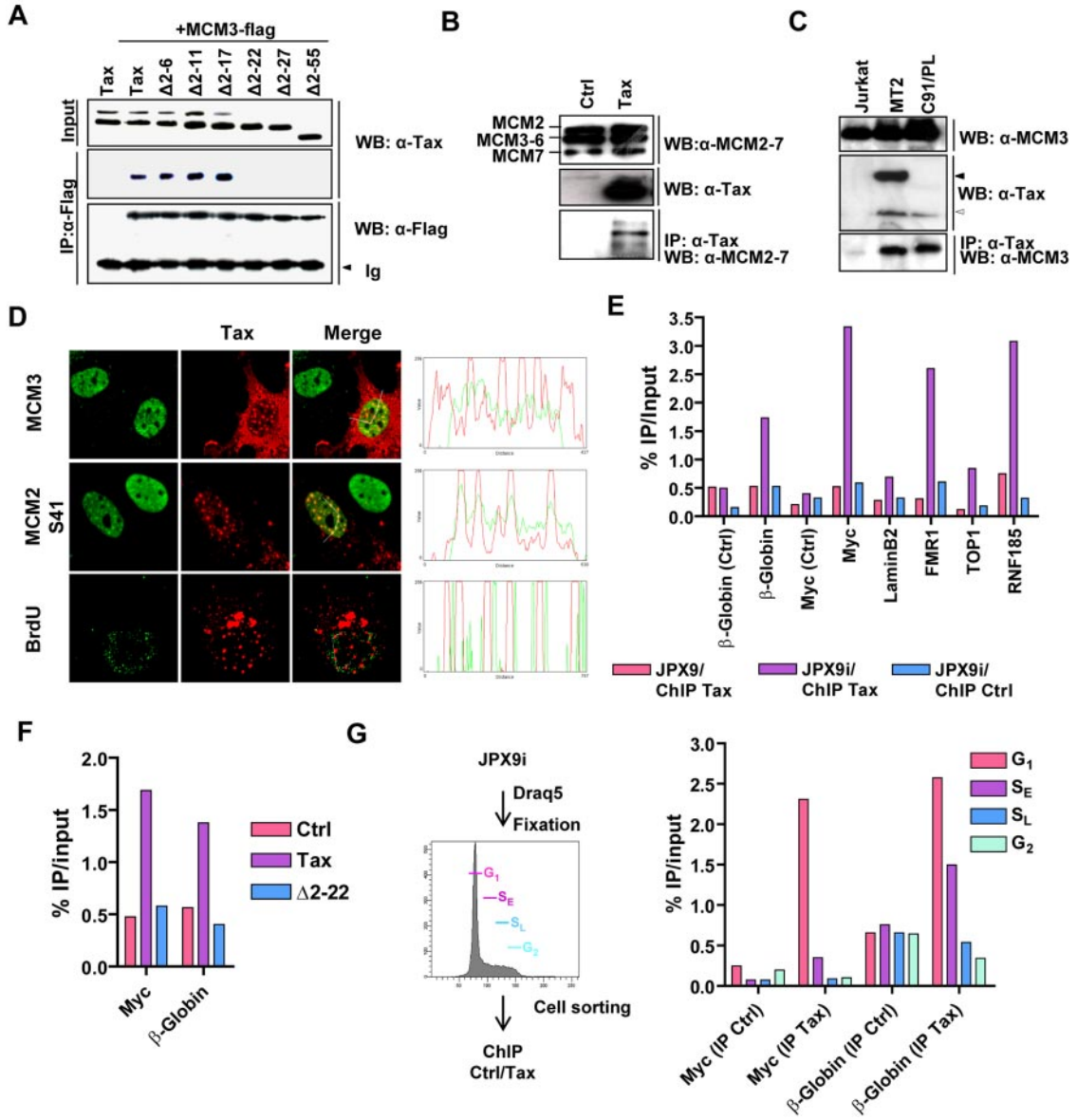

Figure 1. Tax interacts with MCM3. (A) Lysates from HeLa cells transiently transfected with plasmids encoding either wild-type Tax (pSGTax-1) or serial deletion mutants (Δ2-6 to Δ2-55; numbers indicate Tax amino acid residue) and MCM3-Flag protein were subjected to immunoprecipitations using anti-Flag antibody (IP: α-Flag). Protein complexes were immunoblotted with anti-Flag (WB: α-Flag) or anti-Tax (WB: α-Tax) antibodies. (B-C) Tax protein was immunoprecipitated from pSGTax-1–transfected HeLa (B) or Jurkat, MT2, and C91/PL (C) cell lysates, and the protein complexes were analyzed by Western blotting using α-Tax, α-MCM2-7, or MCM3 antibodies. Arrows indicate the position of Tax-Env fusion (black arrow in MT2 cells) and wild-type Tax proteins (open arrow). Representative data of 3 independent experiments are shown. (D) HeLa cells were transfected with the pSGTax-1 vector, incubated during 16 hours, and analyzed by confocal microscopy with the indicated antibodies. In the "BrdU" panel, cells were pulsed with 33μM BrdU for 20 minutes before fixation. (E) Chromatin was prepared from JPX9 or $ZnCl_2$-stimulated JPX9 (JPX9i), and the presence of Tax on β-globin, Myc, LaminB2, TOP1, FMR1, and RNF185 replication origins was detected by ChIP followed by quantitative PCR analysis. Regions located 2 kb 5′ to the β-globin and Myc origins were used as control (Ctrl). (F) HeLa cells were transfected with control (Ctrl) or Tax-expression vectors (pSGTax-1 and pSGΔ2-22) and processed for ChIP experiments, as in panel E. (G) JPX9i were fixed, stained with Draq5, and sorted in G_1, early S (S_E), late S (S_L), and G_2 based on their DNA content. ChIP was performed as in panel E. (E-G) Results were expressed as a percentage of input DNA. Representative results of 1 of 3 independent experiments are shown.

of BrdU labeling within the foci ($P > .05$; Figure 2F). Overall, Tax expression led to a global increase (integrated intensity) of BrdU incorporation ($P < .001$; Figure 2G). BrdU foci are thought to be a cluster of 2 to 10 synchronously firing adjacent replication origins arranged into a replication factory containing DNA replication factors.[28] Our data suggest that Tax fires supplementary clusters at the onset of S phase but does not affect the number of active replicons within active factories or the progression of forks emanating from the origin. Modulation of these 2 parameters would indeed modify the intensity of BrdU foci. Consistently, Tax did not affect the density of active replicons (fork-to-fork distance) and the length of replication forks measured by fiber assay (Figure 2H-I). As control, the CHK1 inhibitor Ucn-01 reduced both intracluster fork spacing and fork length as previously described,[16,27] thereby validating the assay.

Because dormant origins are licensed by an excess of MCM2-7 complexes, it is possible to reduce global licensing by RNA interference without affecting the cell cycle.[16] Consistently, silencing of MCM3 reduced chromatin binding of the MCM2-7 complex (supplemental Figure 3A, see chromatin-bound) without affecting

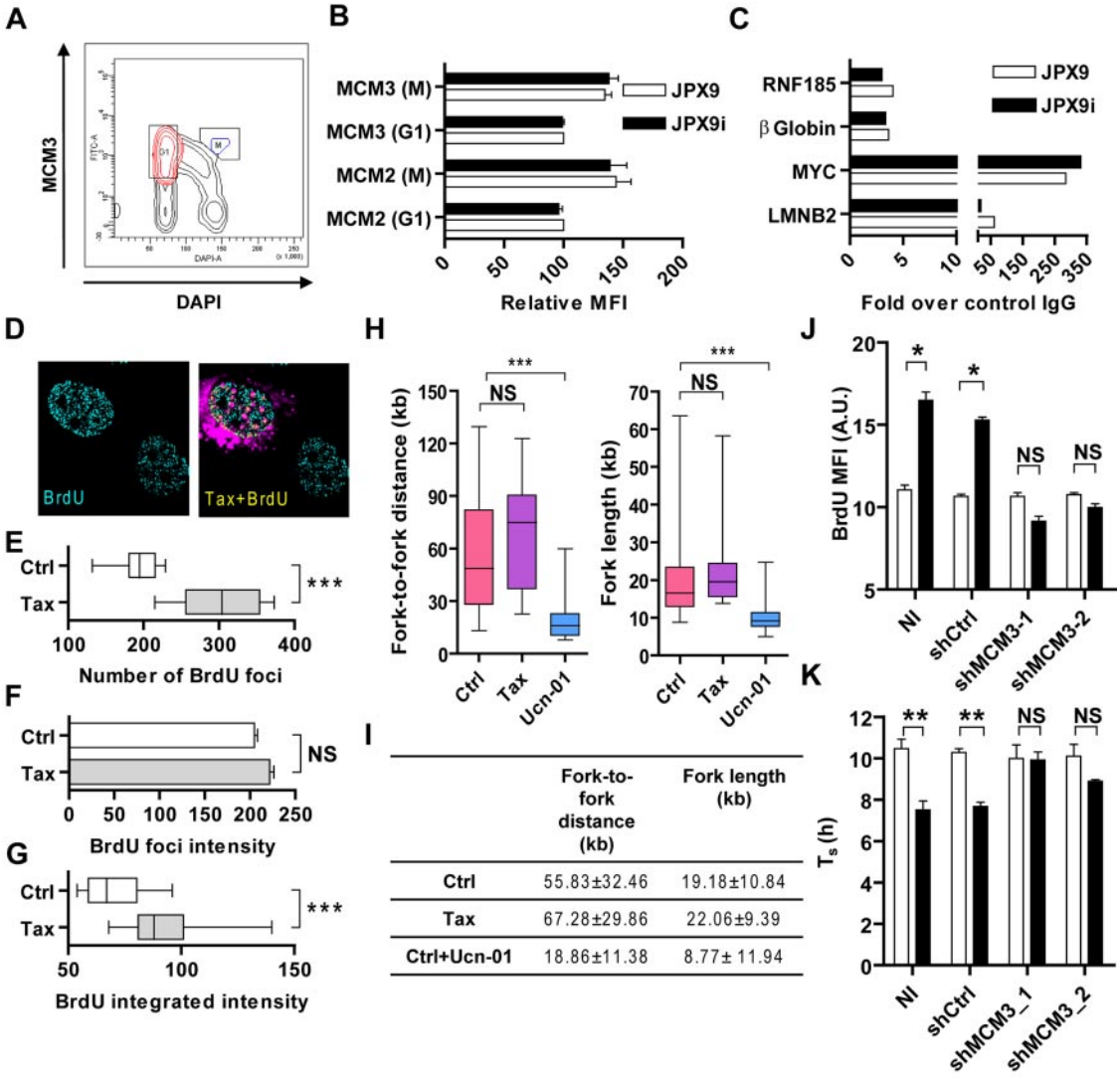

Figure 2. Tax overactivates replication origins. (A-B) JPX9 and JPX9i cells were extracted with CSK buffer, fixed, and stained for MCM2 or MCM3 and DNA content (4′,6-diamidino-2-phenylindole) before flow cytometric analysis. (A) Representative analyses of MCM2 staining and DNA content labeling. (B) MCM2 and MCM3 MFI in G_1 and M phases of the cell cycle normalized to the MFI of control cells in G1 (relative MFI). (C) JPX9 and JPX9i were treated with HU (2.5mM) to synchronize cells at G_1/S transition for 16 hours, and MCM2 occupancy at Myc, LaminB2, β-globin, and RNF185 replication origins was detected by ChIP. Results were expressed as a percentage of input DNA. (B) Representative results of one of 3 independent ChIP experiments are shown. (D) HeLa cells were transfected with a Tax expression vector, incubated during 3 hours, and synchronized at G_1/S transition with 2mM HU. After a short BrdU pulse (15 minutes) in HU-free medium, cells were processed for confocal microscopy. (E) Number of BrdU foci, (F) BrdU foci intensity, and (G) integrated BrdU intensity in control (Ctrl) and Tax-positive cells (n = 50). (H-I) Rat-1 cells stably transduced with control (Ctrl) or Tax-expressing viruses were treated or not with UCN-01 (100nM, 3 hours), pulsed with BrdU (33μM, 30 minutes). DNA was isolated, spread on slides, and the BrdU-labeled tracks were analyzed by confocal microscopy. Next, fork-to-fork distance and length of isolated tracks were measured. (J-K) JPX9 cells were stably transduced with lentiviruses encoding MCM3 shRNAs, stimulated (black bars) or not (open bars) with $ZnCl_2$ (120μM), and pulsed with BrdU for 30 minutes. (J) MFI of BrdU labeling and (K) duration of S phase were analyzed by flow cytometry (see supplemental Figure 4 for details). The results presented are the mean ± SD of 3 independent experiments. A.U. indicates arbitrary units; and NS, not significant. *$P < .05$, according to Kruskal-Wallis test. ***$P < .001$, according to Kruskal-Wallis test.

cell cycle distribution or Tax expression (supplemental Figure 3B-C). Bivariate BrdU/PI flow cytometric analysis in JPX9 cells (as depicted in supplemental Figure 3B) further confirmed that Tax expression increases BrdU incorporation (expressed as BrdU MFI; Figure 2J), but this activity was drastically impaired on MCM3 silencing. This latter result suggests that maximal licensing of replication origins by MCM complexes is required for Tax firing of supplementary origins.

We next examined the impact of supplementary origins firing on global rates of DNA replication. We determined the duration of S and G_2/M phases in unsynchronized cells using bivariate BrdU/PI dot plots during a chase period (supplemental Figure 4). This method estimates the relative movement of BrdU-labeled cells between G_1 and G_2/M using kinetic parameters of defined populations present in different phases of the cell cycle. In JPX9 and Rat-1 cells, the relative movement of BrdU labeled cells was significantly increased on Tax expression (Figure 2K; supplemental Figure 4). Modeling of these data demonstrated that Tax shortens the duration of S phase by 2 hours and that shRNA-mediated reduction of MCM licensing restrained this activity (T_s, Figure 2K). Flow cytometric analysis of cells released from a G_1/S block yielded similar conclusions. Indeed, Tax-expressing cells reached the G_2 phase 2 hours earlier than control cells (supplemental Figure 5). Importantly, the duration of the G_2/M phase ($T_{G2/M}$) was not affected by induction of Tax expression (supplemental Figure 4). Together, these data thus demonstrate that Tax targets MCM2-7 complexes,

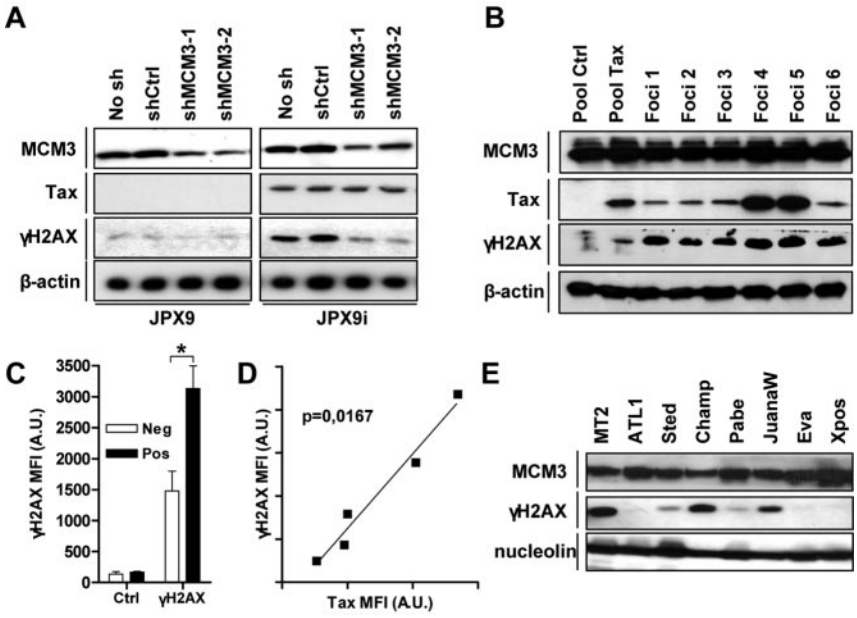

Figure 3. Tax triggers DNA lesions. (A) Lysates recovered from JPX9 cell lines stably transduced with lentiviruses encoding MCM3 shRNAs and stimulated or not with $ZnCl_2$ were analyzed by Western blot using antibodies directed against MCM3, Tax, β-actin, and γH2AX. (B) Cell lysates were prepared from control (Pool ctrl) and Tax (Pool Tax) transduced Rat-1 cells and from 6 soft agar foci (foci 1-6). Immunoblots were performed using indicated antibodies. (C-D) MFI of control (Ctrl), Tax and γH2AX staining in HTLV-1-negative (Jurkat, CEM, HUT78), and infected (MT2, MT4, C91/PL, C8166-45, HUT102) was measured by flow cytometry as described in supplemental Figure 6. Data are the (C) mean of γH2AX staining intensities in HTLV-1 negative (Neg) and positive (Pos) and (D) the correlation between γH2AX and Tax intensities in HTLV-1–infected cells. (E) Lysates from MT2 and various IL-2–dependent HTLV-1–infected cell lines were processed as described in panel B. A.U. indicates arbitrary units. $^*P < .05$.

increases the number of active replicons, and stimulates DNA replication during S phase.

Unscheduled origin firing by Tax generates replicative genomic lesions

Abnormal replication program compromises genome stability by causing replicative DNA damage, such as double-strand breaks (DSBs). DSB induction by Tax was revealed by 2 methods: a TUNEL-based assay (supplemental Figure 6A) and the detection of the phosphorylated form of H2AX (γH2AX; Figure 3A). In both assays, MCM3 silencing decreased the ability of Tax to generate genomic lesions. Kinetic analysis in G_1/S-synchronized HeLa cells further revealed that γH2AX progressively accumulated in Tax-positive cells near S phase completion (supplemental Figure 6B). Caffeine, an inhibitor of ATM and ATR kinases, abrogated γH2AX induction. These data suggest that activation of supplementary origins and progression through cell cycle are required for Tax to generate DSB triggering ATM/ATR-dependent H2AX-phosphorylation.

Finally, we examined the status of H2AX phosphorylation in cells transformed by Tax and HTLV-1. H2AX was hyperphosphorylated in Tax-transformed Rat-1 foci grown in soft agar (Figure 3B). Using flow cytometry, we further observed that the amounts of γH2AX were significantly higher in HTLV-transformed cells compared with negative cell lines (supplemental Figure 6C; Figure 3C) and correlated ($P = .0167$, Spearman test) with the level of Tax expression in infected cells (Figure 3D). Phosphorylation of H2AX was also detected in IL-2–dependent cell lines derived from HTLV-1–infected patients (Figure 3E). By increasing the number of active origins, Tax thus appears to compromise genome stability.

Interaction with MCM and p300 is required for Tax-mediated unscheduled origin activation

Replication domains are activated according to a precise spatiotemporal program orchestrated by SPK (CDK2 and CDC7) and histone-modifying enzymes, whereas origins firing within a cluster depends on ATR/CHK1 kinases.[29,30] Establishment of this timing program occurs in early G_1, at a stage called "timing decision point" that coincides with positioning of subchromosomal domains in euchromatin or in heterochromatin. Our data suggest that Tax fires supplementary replication factories but does not change the distribution of origins within active factories. Importantly, Tax is known to modulate CDK function through direct binding and transcriptional activation/repression and to associate with histone acetyltransferases (HAT) and deacetylases.[10] To clarify the mechanisms of Tax-induced unscheduled activation of origins, we examined BrdU incorporation in cells expressing a set of Tax mutants and released from a G_1/S block. Mutation M22 is known to abrogate the ability of Tax to affect CDK function, whereas M47 and K88A fail to bind P/CAF and CBP/p300 HATs, respectively.[10] On the other hand, these 3 latter mutants, but not Δ2-22, interacted with MCMs (supplemental Figure 7). Because only M22 and M47 retained their ability to increase BrdU incorporation (Figure 4A), our data indicate that Tax fires supplementary replication factories through a CBP/p300-dependent, but CDK-independent, mechanism. CDC7 and CDK1-2 trigger origin activation at least in part via phosphorylation of MCM2 at serines 27, 41, and 108.[31] Using flow cytometry, we showed that Tax expression in JPX9 cells did not change phosphorylation levels of chromatin-bound MCM2 during G_1 phase (ie, when timing is programmed; supplemental Figure 8; Figure 4B). In contrast, Tax stimulated histone H3 acetylation at known p300 substrates: lysines 9, 14, and 56. Similarly, wild-type Tax raised levels of acetylated H3K56 in G_1/S synchronized fibroblasts, whereas the K88A mutant lacked this activity (supplemental Figure 9; Figure 4C). These observations are consistent with a mechanism of Tax-dependent activation of supplementary origins through a HAT-dependent process.

Early-replicating domains are characterized by the presence of HATs and acetylated histones, whereas late firing origins correlate with a histone deacetylation pattern. Therefore, we studied p300 and acetylated histone H3 occupancy by ChIP on previously characterized early (LaminB2 and Myc) and late (β-globin and RNF185) replication origins on Tax expression. Compared with late origins, early origins were associated with higher levels of p300, H3K9-14ac, and H3K56ac (Figure 4D), p300, H3K9-14ac, and H3K56ac panels (white bars), as described in the literature.[32,33]

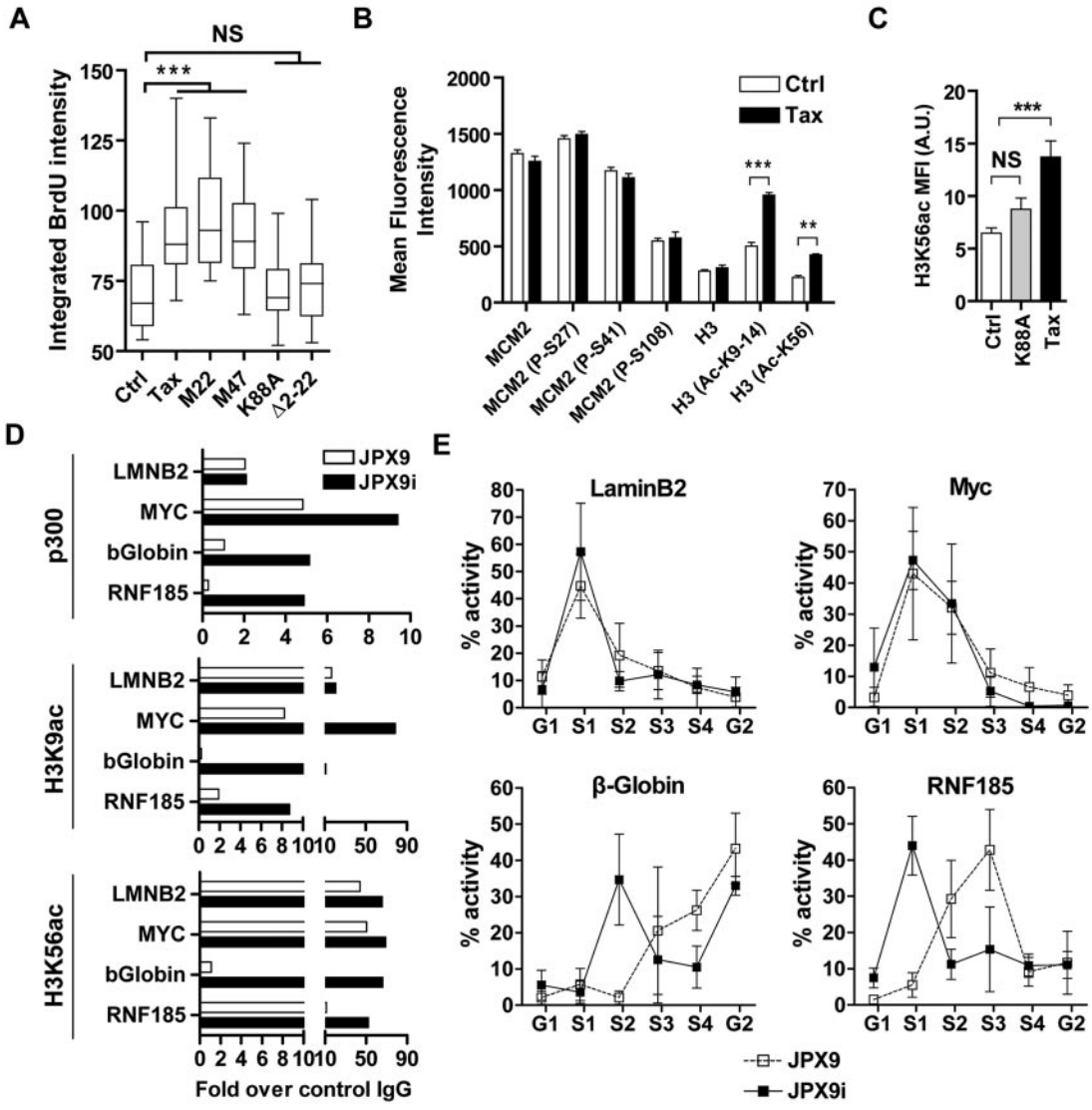

Figure 4. Tax cooperates with p300 to induce histone hyperacetylation at late origins. (A) HeLa cells were transfected with different Tax expression vectors (wild-type Tax, M22, M47, K88A, and Δ2-22) and synchronized at G_1/S transition with HU. Ctrl corresponds to cells transfected with an empty vector. BrdU incorporation was performed as described in Figure 2D. (B) JPX9 and JPX9i cells were treated with CSK buffer and then fixed and analyzed by confocal microscopy using indicated antibodies. Fluorescence intensity of cells in G_1 was measured as described in supplemental Figure 8. (C) Rat-1 cells were transfected with expression vectors for wild-type Tax or K88A mutant and synchronized at G_1/S transition with HU before CSK extraction, fixation, and confocal microscopy analysis using α-H3K56ac and α-Tax antibodies (see supplemental Figure 9). Mean fluorescence intensity of H3K56ac labeling was analyzed in control (Ctrl), wild-type Tax, or mutant K88A-positive cells (n = 30). (D) p300, H3K9-14ac, and H3K56ac occupancy at Myc, LaminB2, β-globin, and RNF185 replication origins was detected by ChIP in JPX9 cells. ChIP results were expressed as a percentage of input DNA. Representative results of 1 of 3 independent ChIP experiments are shown. (E) Replication timing analysis at Myc, LaminB2, β-globin, and RNF185 replication origins was determined by isolation of nascent DNA in JPX9 (■) or JPX9i cells (□) sorted in G_1, $S_{1\text{-}4}$, and G_2 stages of the cell cycle. NS indicates not significant. $^{**}P < .01$, $^{***}P < .001$, according to Kruskal-Wallis test.

Although Tax only marginally affected p300, H3K9-14ac, and H3K56ac occupancy at early origins, it drastically increased their recruitment at late origins. In other terms, our data demonstrate that Tax promotes recruitment of p300 and hyperacetylates histone H3 at late replication origins.

To determine whether Tax-mediated hyperacetylation of late replication origins affects the temporal program of replication timing, asynchronous BrdU-pulsed JPX9 cells were sorted into 6 cell-cycle fractions according to DNA content, and nascent DNA was isolated by BrdU immunoprecipitation (Figure 4E). The abundance of sequences overlapping LaminB2, Myc, β-globin, and RNF185 origins within newly replicated DNA was then determined by PCR. In control cells, the LaminB2 and Myc origins' activity peaked within the first half of S phase, unlike β-globin and RNF185 genes for which maximal activity was observed in late S. These results thus confirm that LaminB2 and Myc genes are early replication origins, whereas β-globin and RNF185 regions contain a late origin of replication. Very interestingly, although Tax expression did not affect LaminB2 and Myc replication origin activity, it advanced β-globin and RNF185 replication timing from late to early.

Together, our data thus show that unscheduled origin firing by Tax at G_1/S transition correlates with post-transcriptional modifications of chromatin at origins and changes in replication timing.

Discussion

We have described here a mechanism that links the HTLV-1 Tax oncoprotein with the minichromosome maintenance complex and

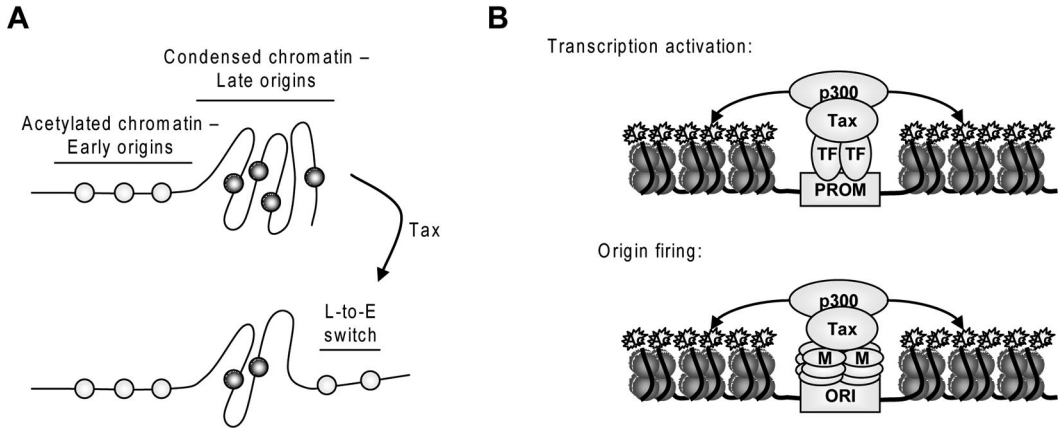

Figure 5. Mechanism of Tax-induced overactivation of replication origins. (A) Accessibility of chromatin dictates the fate of replication origins. Acetylated chromatin replicates early in S phase, whereas more condensed chromatin replicates later in S phase. Tax-mediated acetylation of late origins increases chromatin accessibility and provokes a late-to-early switch of replication timing. (B) Similarities between the mechanisms of transcriptional activation and origin firing: Tax forms complexes with transcription factors (TF) or MCM proteins (M) and p300, leading to histone acetylation at gene promoters (PROM) and replication origins (ORI), respectively.

provide evidence of its biologic relevance in the context of HTLV-1 persistence and pathogenesis. We have demonstrated that Tax favors replication origin firing, accelerates S phase progression, and leads to DNA damage in a MCM2-7 and p300-dependent manner. These 3 interconnected mechanisms provide a mechanistic rationale for the process of clonal expansion of HTLV-1–infected cells as well as for genomic DNA alterations characteristic of development of ATL.

Current views indeed consider that HTLV-1 persistence relies on pro-proliferative activities of Tax and subsequent clonal expansion of infected cells.[2,5] Among these activities, Tax stimulates G_1 to S transition through cyclin/CDK complex activation, suppresses the activity of negative cell-cycle regulators, such as p53, $p16^{INK4A}$, and $p27^{KIP1}$, CHK1-2, and ATM,[8] and favors cell survival under stressful conditions.[34] On the other hand, cell dynamic experiments revealed that Tax-expressing infected T cells incorporate higher levels of nucleotide analogs compared with control cells during a pulse period,[2,35] strongly indicating that increased proliferation of infected cells relies, at least in part, on increased DNA replication rates. Even if other viral proteins could play a role in this process, we now demonstrate that the interplay between Tax and replication origins stimulates DNA synthesis and progression through the S phase, thereby providing molecular insights into the mechanisms involved in clonal expansion of HTLV-1–infected cells.

A long-standing paradox is why oncogenes provide proliferative advantages to cells while triggering cell cycle arrest and senescence. Combining a wide range of pro-mitotic and antiproliferative activities, Tax is apparently no exception. Several reports indeed demonstrated that Tax-expressing cells undergo ATM/ATR-dependent cell cycle delay in S-G_2 phases, G_1 arrest, and senescence because of a surge of $p21^{Waf1/Cip1}$ expression, or even apoptosis.[36-40] Although these observations appear contradictory with the ability of Tax to speed up S phase progression, several lines of evidence suggest that pro-mitotic and antiproliferative activities have to be considered as interconnected processes. Indeed, the ATM/ATR-dependent phosphorylation of H2AX in Tax-expressing cells suggests that unscheduled activation of replication origins creates replicative lesions that alarm the DDR machinery. Restraining the capacity of Tax to fire supplementary origins and to accelerate S phase progression decreased DSB induction and DDR pathway engagement. As activation of this pathway causes a fraction of Tax-expressing cells to halt cell cycle,[36] our data strengthen the link between Tax-induced enforced proliferation and DNA-damaging activities leading to cell-cycle arrest. Recent studies also suggest that DNA damage and H2AX phosphorylation in Tax-expressing cells result from induction of reactive oxygen species[9] and/or sequestration of DDR-associated proteins in TSS.[41-43] It thus appears that several Tax activities contribute to DSB formation and DDR pathway engagement. Finally, whereas DDR activation would be detrimental for viral persistence, our data (M.B. et al, manuscript in preparation) rather suggest that a phenomenon of checkpoint adaptation, similar to that observed in human tumors,[44] occurs in the course of HTLV-1 infection, allowing cells to evade DDR-induced cell cycle arrest, to accumulate genomic DNA alterations, and to progress toward ATL.

Accessibility of chromatin dictates the fate of replication origins.[45] Early replication takes place within the euchromatic compartment of the nucleus, whereas late replication occurs at nuclear and nucleolar peripheries and in heterochromatin blocks. Although replication timing is mitotically stable and inherited through multiple cell cycles, dynamic changes are frequently observed during cell differentiation and coincide with changes in higher-order organization of the genome and transcriptional activity.[45] CDKs and ATR/Chk1 kinases have also been demonstrated to play a role in the activation of replication factories and dormant origins within active factories, respectively.[17,27] In this report, we have provided evidence that Tax activates supplementary replication factories at the onset of S phase. Figure 5A is consistent with a mechanism in which Tax interaction with p300 and histone hyperacetylation at late replication origins causes a shift to early replication. Indeed, Tax advances β-globin and RNF185 replication but does not affect the timing of other late origins, such as FMR1 (also called FRAXA) replication (data not shown), suggesting that Tax does not switch replication timing of all origins. Noteworthy, it has been recently demonstrated that p300 recruitment at β-globin locus regulates usage of this origin.[46] Overall, our data suggest that Tax-mediated firing of replication origins and activation of gene transcription rely on similar mechanisms that require HAT recruitment and histone acetylation at origins of replication and gene promoters, respectively (Figure 5B). Tax recruits a plethora of transcription factors within speckled structures to activate transcription while DNA accumulates at the surface of TSS.[47] We now show that these structures are enriched in phosphorylated forms of MCM2 and in close vicinity to the active

replication origins. TSS could thus play an unanticipated role in DNA replication and act as a platform for DNA transactions.

In conclusion, we describe here an unanticipated mechanism by which Tax modulates replication timing and fires supplementary origins. Because replication timing is stably inherited through multiple mitoses, transient Tax expression could therefore affect genome organization during several cell cycles. This "hit-and-run" process could favor mitotic expansion of the infected clone in the absence of continuous Tax expression, allowing escape from the host immune response.

Acknowledgments

The authors thank Ralph Grassmann and Kirsten Fraedrich for providing cell lysates; Masahiro Fujii, David Cortez, and Marc Vidal for expression vectors; Françoise Bex for monoclonal antibodies; Charles Bangham for helpful comments and critical reading of the manuscript; and Jean-Rock Jacques, Carole François, and Jean-François Dewulf for technical help.

This work was supported by the Fonds National de la Recherche Scientifique, the Télévie, the Belgian Foundation against Cancer, the Sixth Research Framework Program of the European Union (project INCA LSHC-CT-2005-018704), the Neoangio excellence program and the Partenariat Public Privé PPP INCA of the Direction générale des Technologies, de la Recherche et de l'Energie/DG06 of the Walloon government, the Action de Recherche Concertée Glyvir of the Communauté française de Belgique, the Fonds spéciaux pour la Recherche of the University of Liège, the Synbiofor program of GxABTUL (University of Liège), the Center anticancéreux près University of Liège, and the Plan Cancer of the Service Public Fédéral. All authors are members of the FRS-FNRS.

Authorship

Contribution: M.B. and L.W. designed the experiments and wrote the manuscript; M.B. performed experiments and analyzed data; S.L. and J.-C.T. provided plasmids and performed yeast 2-hybrid screening and coimmunoprecipitation experiments; and S.L., J.-C.T., and R.K. gave conceptual advice.

Conflict-of-interest disclosure: The authors declare no competing financial interests.

Correspondence: Luc Willems, National Fund for Scientific Research, Gembloux Agro-Bio Tech, Molecular and Cellular Biology, University of Liège, Belgium, 13 avenue Maréchal Juin, 5030 Gembloux, Belgium; e-mail: luc.willems@ulg.ac.be.

References

1. Proietti FA, Carneiro-Proietti AB, Catalan-Soares BC, Murphy EL. Global epidemiology of HTLV-I infection and associated diseases. *Oncogene.* 2005; 24(39):6058-6068.
2. Asquith B, Zhang Y, Mosley AJ, et al. In vivo T lymphocyte dynamics in humans and the impact of human T-lymphotropic virus 1 infection. *Proc Natl Acad Sci U S A.* 2007;104(19):8035-8040.
3. Asquith B, Bangham CR. How does HTLV-I persist despite a strong cell-mediated immune response? *Trends Immunol.* 2008;29(1):4-11.
4. Matsuoka M, Jeang KT. Human T-cell leukaemia virus type 1 (HTLV-1) infectivity and cellular transformation. *Nat Rev Cancer.* 2007;7(4):270-280.
5. Boxus M, Willems L. Mechanisms of HTLV-1 persistence and transformation. *Br J Cancer.* 2009; 101(9):1497-1501.
6. Lemoine FJ, Marriott SJ. Accelerated G(1) phase progression induced by the human T cell leukemia virus type I (HTLV-I) Tax oncoprotein. *J Biol Chem.* 2001;276(34):31851-31857.
7. Haller K, Wu Y, Derow E, et al. Physical interaction of human T-cell leukemia virus type 1 Tax with cyclin-dependent kinase 4 stimulates the phosphorylation of retinoblastoma protein. *Mol Cell Biol.* 2002;22(10):3327-3338.
8. Marriott SJ, Semmes OJ. Impact of HTLV-I Tax on cell cycle progression and the cellular DNA damage repair response. *Oncogene.* 2005;24(39): 5986-5995.
9. Kinjo T, Ham-Terhune J, Peloponese JM Jr, Jeang KT. Induction of reactive oxygen species by human T-cell leukemia virus type 1 tax correlates with DNA damage and expression of cellular senescence marker. *J Virol.* 2010;84(10):5431-5437.
10. Boxus M, Twizere JC, Legros S, et al. The HTLV-1 Tax interactome. *Retrovirology.* 2008;5: 76.
11. Semmes OJ, Jeang KT. Localization of human T-cell leukemia virus type 1 tax to subnuclear compartments that overlap with interchromatin speckles. *J Virol.* 1996;70(9):6347-6357.
12. Lodewick J, Lamsoul I, Bex F. Move or die: the fate of the tax oncoprotein of HTLV-1. *Viruses.* 2011;3(6):829-857.
13. Pichler K, Kattan T, Gentzsch J, et al. Strong induction of 4-1BB, a growth and survival promoting costimulatory receptor, in HTLV-1-infected cultured and patients' T cells by the viral tax oncoprotein. *Blood.* 2008;111(9):4741-4751.
14. Azuara V. Profiling of DNA replication timing in unsynchronized cell populations. *Nat Protoc.* 2006;1(4):2171-2177.
15. Jackson DA, Pombo A. Replicon clusters are stable units of chromosome structure: evidence that nuclear organization contributes to the efficient activation and propagation of S phase in human cells. *J Cell Biol.* 1998;140(6):1285-1295.
16. Ge XQ, Jackson DA, Blow JJ. Dormant origins licensed by excess Mcm2-7 are required for human cells to survive replicative stress. *Genes Dev.* 2007;21(24):3331-3341.
17. Thomson AM, Gillespie PJ, Blow JJ. Replication factory activation can be decoupled from the replication timing program by modulating Cdk levels. *J Cell Biol.* 2010;188(2):209-221.
18. Terry NH, White RA. Flow cytometry after bromodeoxyuridine labeling to measure S and G2+M phase durations plus doubling times in vitro and in vivo. *Nat Protoc.* 2006;1(2):859-869.
19. White RA, Meistrich ML, Pollack A, Terry NH. Simultaneous estimation of T(G2+M), T(S), and T(pot) using single sample dynamic tumor data from bivariate DNA-thymidine analogue cytometry. *Cytometry.* 2000;41(1):1-8.
20. Fryrear KA, Durkin SS, Gupta SK, Tiedebohl JB, Semmes OJ. Dimerization and a novel Tax speckled structure localization signal are required for Tax nuclear localization. *J Virol.* 2009;83(11): 5339-5352.
21. Tsuji T, Sheehy N, Gautier VW, et al. The nuclear import of the human T lymphotropic virus type I (HTLV-1) tax protein is carrier- and energy-independent. *J Biol Chem.* 2007;282(18):13875-13883.
22. Blow JJ, Dutta A. Preventing re-replication of chromosomal DNA. *Nat Rev Mol Cell Biol.* 2005; 6(6):476-486.
23. Machida YJ, Hamlin JL, Dutta A. Right place, right time, and only once: replication initiation in metazoans. *Cell.* 2005;123(1):13-24.
24. Tsuji T, Ficarro SB, Jiang W. Essential role of phosphorylation of MCM2 by Cdc7/Dbf4 in the initiation of DNA replication in mammalian cells. *Mol Biol Cell.* 2006;17(10):4459-4472.
25. Montagnoli A, Valsasina B, Brotherton D, et al. Identification of Mcm2 phosphorylation sites by S-phase-regulating kinases. *J Biol Chem.* 2006; 281(15):10281-10290.
26. Friedrich TD, Bedner E, Darzynkiewicz Z, Lehman JM. Distinct patterns of MCM protein binding in nuclei of S phase and rereplicating SV40-infected monkey kidney cells. *Cytometry A.* 2005;68(1):10-18.
27. Ge XQ, Blow JJ. Chk1 inhibits replication factory activation but allows dormant origin firing in existing factories. *J Cell Biol.* 2010;191(7):1285-1297.
28. Gillespie PJ, Blow JJ. Clusters, factories and domains: the complex structure of S-phase comes into focus. *Cell Cycle.* 2010;9(16):3218-3226.
29. Groth A. Replicating chromatin: a tale of histones. *Biochem Cell Biol.* 2009;87(1):51-63.
30. Remus D, Diffley JFX. Eukaryotic DNA replication control: lock and load, then fire. *Curr Opin Cell Biol.* 2009;21(6):771-777.
31. Charych DH, Coyne M, Yabannavar A, et al. Inhibition of Cdc7/Dbf4 kinase activity affects specific phosphorylation sites on MCM2 in cancer cells. *J Cell Biochem.* 2008;104(3):1075-1086.
32. Lucas I, Palakodeti A, Jiang Y, et al. High-throughput mapping of origins of replication in human cells. *EMBO Rep.* 2007;8(8):770-777.
33. Lee TJ, Pascuzzi PE, Settlage SB, et al. Arabidopsis thaliana chromosome 4 replicates in two phases that correlate with chromatin state. *Plos Genet.* 2010;6(6).
34. Legros S, Boxus M, Gatot JS, et al. The HTLV-1 Tax protein inhibits formation of stress granules by interacting with histone deacetylase 6. *Oncogene.* 2011;30(38):4050-4062.
35. Sibon D, Gabet AS, Zandecki M, et al. HTLV-1 propels untransformed CD4 lymphocytes into the

cell cycle while protecting CD8 cells from death. *J Clin Invest.* 2006;116(4):974-983.

36. Haoudi A, Daniels RC, Wong E, Kupfer G, Semmes OJ. Human T-cell leukemia virus-I tax oncoprotein functionally targets a subnuclear complex involved in cellular DNA damage-response. *J Biol Chem.* 2003;278(39):37736-37744.
37. Liang MH, Geisbert T, Yao Y, Hinrichs SH, Giam CZ. Human T-lymphotropic virus type 1 oncoprotein tax promotes S-phase entry but blocks mitosis. *J Virol.* 2002;76(8):4022-4033.
38. Kuo YL, Giam CZ. Activation of the anaphase promoting complex by HTLV-1 tax leads to senescence. *EMBO J.* 2006;25(8):1741-1752.
39. Zhang L, Zhi H, Liu M, Kuo YL, Giam CZ. Induction of p21(CIP1/WAF1) expression by human T-lymphotropic virus type 1 Tax requires transcriptional activation and mRNA stabilization. *Retrovirology.* 2009;6:35.
40. Kasai T, Jeang KT. Two discrete events, human T-cell leukemia virus type I Tax oncoprotein expression and a separate stress stimulus, are required for induction of apoptosis in T-cells. *Retrovirology.* 2004;1:7.
41. Belgnaoui SM, Fryrear KA, Nyalwidhe JO, Guo X, Semmes OJ. The viral oncoprotein tax sequesters DNA damage response factors by tethering MDC1 to chromatin. *J Biol Chem.* 2010;285(43):32897-32905.
42. Gupta SK, Guo X, Durkin SS, et al. Human T-cell leukemia virus type 1 Tax oncoprotein prevents DNA damage-induced chromatin egress of hyperphosphorylated Chk2. *J Biol Chem.* 2007;282(40):29431-29440.
43. Durkin SS, Guo X, Fryrear KA, et al. HTLV-1 tax oncoprotein subverts the cellular DNA damage response via binding to DNA-dependent protein kinase. *J Biol Chem.* 2008;283(52):36311-36320.
44. Bartek J, Lukas J. DNA damage checkpoints: from initiation to recovery or adaptation. *Curr Opin Cell Biol.* 2007;19(2):238-245.
45. Hiratani I, Gilbert DM. Replication timing as an epigenetic mark. *Epigenetics.* 2009;4(2):93-97.
46. Karmakar S, Mahajan MC, Schulz V, Boyapaty G, Weissman SM. A multiprotein complex necessary for both transcription and DNA replication at the beta-globin locus. *EMBO J.* 2010;29(19):3260-3271.
47. Baydoun H, Duc-Dodon M, Lebrun S, Gazzolo L, Bex F. Regulation of the human T-cell leukemia virus gene expression depends on the localization of regulatory proteins Tax, Rex and p30II in specific nuclear subdomains. *Gene.* 2007;386(1):191-201.